*J. Fluid Mech.* (1972), *vol.* 54, *part* 1, *pp.* 19–38
*Printed in Great Britain*


# Turbulent non-equlibrium wakes

By A. PRABHU AND R. NARASIMHA†
Department of Aeronautical Engineering, Indian Institute of Science, Bangalore

(Received 15 September 1971)

We consider here the detailed application of a model Reynolds stress equation (Narasimha 1969) to plane turbulent wakes subjected to pressure gradients. The model, which is a transport equation for the stress exhibiting relaxation and diffusion, is found to be consistent with the observed response of a wake to a nearly impulsive pressure gradient (Narasimha & Prabhu 1971). It implies in particular that a wake can be in equilibrium only if the longitudinal strain rate is appreciably less than the wake shear.

We then describe a further series of experiments, undertaken to investigate the range of validity of the model. It is found that, with an appropriate convergence correction when necessary, the model provides excellent predictions of wake development under favourable, adverse and mixed pressure gradients. Furthermore, the behaviour of constant-pressure distorted wakes, as reported by Keffer (1965, 1967), is also explained very well by the model when account is taken of the effective flow convergence produced by the distortion. In all these calculations, only a simple version of the model is used, involving two non-dimensional constants both of which have been estimated from a single relaxation experiment.

## 1. Introduction

This paper is an attempt to provide a quantitative description of the development of plane turbulent wakes subjected to arbitrary pressure gradients. Such an attempt, unless restricted to very small pressure gradients, will have to take account of the strong influence of the history of the flow implied in the observed behaviour of a relaxing wake (Narasimha & Prabhu (1972), hereafter referred to as I). Models for the Reynolds stress that allow for a relaxation effect (e.g Nee & Kovasznay 1969; Nash & Hicks 1969) have usually been formulated for turbulent boundary layers and (without further modification) are likely to be useful for wakes only for relatively short distances downstream of the trailing edge (Bradshaw 1969).

We adopt and study here a model (Narasimha 1969) which was proposed in the light of the experiments on wakes reported in I, but which is capable of generalization, especially to boundary layers with a wake-like outer layer. Our aim here is not to represent each term of the stress equation as Bradshaw, Ferriss & Atwell (1967) have done for the energy equation, but rather to model the overall behaviour of the terms taken together. The model is relatively simple, and can

† Present address: Department of Mathematics, University of Strathclyde, Glasgow.

handle in a natural way flow situations involving stresses of opposite sign. It involves only two coefficients, one of which is related to the relaxation characteristics of the flow and the other to equilibrium properties. As the scaling laws for these parameters can be easily obtained, suitable non-dimensional numbers nvolving them can (in the simplest version of the model) be taken as constants.

When preliminary work showed that this model provided an excellent description of wake development in a nearly impulsive pressure gradient, further experiments were undertaken with a view to providing more severe test cases for the model. For convenience, these are reported briefly in § 2 before the model adopted is studied. Other experiments which turn out to be relevant to a consideration of non-equilibrium effects are those on strained and distorted wakes studied by Reynolds (1962) and Keffer (1965, 1967). Although these studies were seeking self-preserving solutions the experiments (especially those of Keffer) often revealed no trend towards equilibrium, and therefore fall within the scope of the analysis to be described below.

In § 3 we briefly describe the basis for the model adopted, its consistency with the observations in I, and the implications for equilibrium flows. A method of solving the equations is described in § 4. We then undertake (in § 5) a detailed comparison of the flow development predicted by the model with all the available experimental data. A concluding discussion is presented in § 6.

## 2. The experiments

A total of six different series of experiments, each with a different pressure gradient, were conducted. Some relevant details regarding each series are summarized in table 1. When naming the experiments, we use the letters F, M and A to denote favourable, mixed and adverse pressure gradients respectively. Flows F 1 and F 2 have already been reported in I but are included in table 1 for completeness. The instrumentation used for the measurements was the same as in I.

### 2.1. *The wind tunnels*

Two different tunnels were used in the course of this work; the configurations are shown in figure 1. The 'one-foot' tunnel has a test section which is $1 \times 1 \times 14$ ft.; the unusual length (found necessary for attainment of the final equilibrium state in F 2) meant that strictly two-dimensional flow was not possible far downstream along the test section, and we have been forced to apply certain convergence corrections, described in the appendix. The maximum speed possible in the tunnel is 120 ft/s. All experiments involving short favourable pressure gradients were conducted in this tunnel.

For obtaining short adverse pressure gradients, the $4 \times 9$ in. tunnel shown in figure 1 (*b*) was used. Separation of the tunnel wall boundary layer due to the adverse gradient was avoided by boundary-layer control using blowing. The suppression of separation was confirmed by tuft surveys and by measurements of the pressure distribution.

Figure 1 (*c*) shows the twin-plate wake generator used in most of the experiments.

| Experiment | Tunnel | Wake generator | $U_1$ (ft/s) | Extreme $\lambda$ ($\lambda = U'\delta/w_0$) | Maximum $\lvert\lambda w_0/U\rvert$ | Nature of pressure gradient |
|---|---|---|---|---|---|---|
| F 1 | 1 × 1 ft | Twin-plate | 64·0 | +0·045 | 0·00197 | Impulsive favourable |
| F 2 (*a*) | 1 × 1 ft | Twin-plate | 37·2 | — | — | Impulsive favourable |
| F 2 (*b*) ≡ F 2 | 1 × 1 ft | Twin-plate | 64·6 | +0·119 | 0·0054 | Impulsive favourable |
| F 2 (*c*) | 1 × 1 ft | Twin-plate | 80·8 | — | — | Impulsive favourable |
| F 3 | 1 × 1 ft | Twin-plate | 57·6 | +0·35 | 0·01125 | Impulsive favourable |
| F 4 | 1 × 1 ft | Circular cylinder | 47·6 | +1·57 | 0·0122 | Continuous favourable |
| A 1 | 4 × 9 in. | Twin-plate | 78·5 | −0·186 | 0·0144 | Impulsive adverse |
| M 1 | 1 × 1 ft | Twin-plate | 64·5 | +0·258<br>−0·152 | 0·0111<br>— | Favourable followed by adverse |

TABLE 1. List of experiments

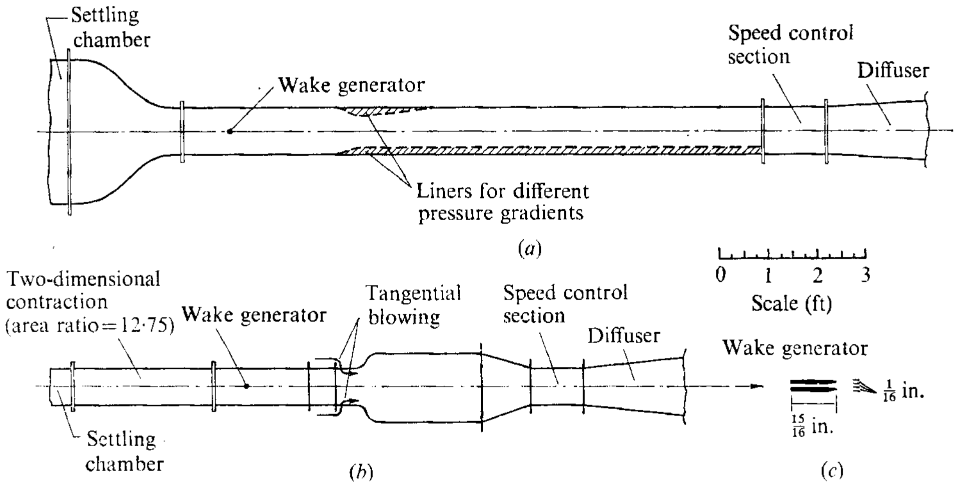


FIGURE 1. (*a*) The 'one-foot' tunnel. Two typical liners (each used in a different experiment) are also shown. (*b*) The 4 × 9 in. tunnel, used for obtaining impulsive adverse pressure gradients with the help of boundary-layer control by blowing on the side walls. The wind velocity in either tunnel can be varied by the operation of flaps in the speed control section. (*c*) The twin-plate wake generator used in most of the experiments reported here.

### 2.2. *The pressure gradients*

The free-stream velocity distributions $U(x)$ in the different experiments listed in table 1 are all shown in figure 2. Of these, the distributions F 1, F 2, F 3 and A 1 were designed to approximate step-function changes in $U$ (corresponding to near delta functions in the pressure gradient) without, however, violating the boundary-layer approximation (see discussion in I). The pressure gradients for all the experiments conducted in the one-foot tunnel were obtained by placing suitable liners on the side walls, as indicated for two typical cases in figure 1 (*a*). In the experiments F 1, F 2 and F 3 the liners produced a contraction in the tunnel cross-sectional area over a distance of about 6 in., after which the liner thickness remained constant until the end of the test section. A divergence on the other two tunnel walls corrected for the effect of boundary-layer growth.

The adverse pressure gradient A 1 was created by an expansion of the test section of the 9 × 4 in. tunnel to 17 × 4 in. over a distance of 6 in.

The results of the experiments are shown together with those of the theory we shall describe below in figures 4–10.

## 3. Model for stress transport

### 3.1. *The equation*

The basis of the model we shall adopt here (Narasimha 1969) is briefly the assumption that each of the terms in the exact but insoluble stress transport equation (for $d\tau/dt$) may always be considered as the sum of its value at a suitably defined local equilibrium state (to be discussed in § 3.3) and a non-equilibrium perturbation. The latter can, in view of the exponential approach to equilibrium noted in I, be taken as proportional to the deviation of the stress from the local equilibrium

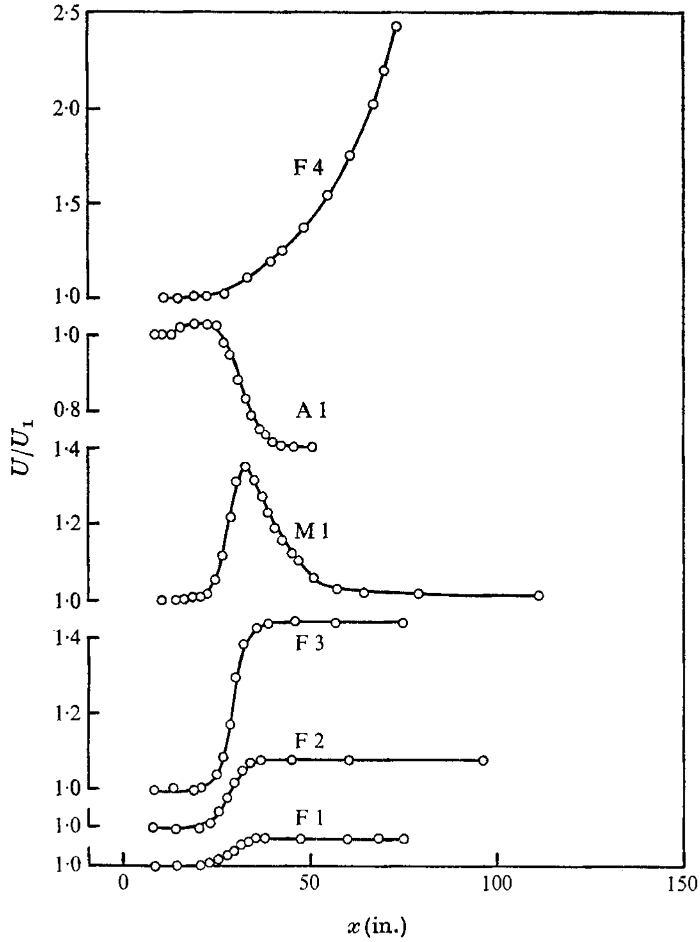


FIGURE 2. Free-stream velocity distributions in the present experiments.

value $\bar{\tau}$, at least in a first approximation for small departures. The net non-equilibrium contribution to stress transport is therefore of the form $A(\bar{\tau}-\tau)$. The equilibrium transport terms, characterizing an effectively memory-less and parabolic flow, are modelled as being *collectively* equivalent to gradient diffusion in the stress. This is certainly consistent with observed stress distributions in many equilibrium flows, including the wake, where the well-known dipole solution of the diffusion equation applies (see Narasimha 1969). The model equation for stress transport is

$$\frac{d\tau}{dt} = A(\bar{\tau}-\tau) + \frac{\partial}{\partial y}\left(\nu_\tau \frac{\partial \tau}{\partial y}\right), \tag{3.1}$$

where $\nu_\tau$ is the stress diffusivity. It is worth emphasizing that the concept of collective modelling implies that the terms in (3.1) should not individually be identified with those of the exact transport equation. For example, the term $A\tau$ in (3.1) does *not* represent stress production but contains a part of it, as do the rest of the terms.

Further extensions to the model are suggested by refinements of the argument we have sketched here (and will be considered in a future paper by Narasimha) but we shall find below that, for such purposes as describing the mean flow development in wakes, it is not even necessary to consider the (expected) dependence of $A$ and $\nu_\tau$ on the stress, velocity and position. Instead, the simplest assumption of taking suitable non-dimensional forms of $A$ and $\nu_\tau$ to be constant turns out to be more than adequate for all flows considered here. Indeed, from the results of I, the relaxation time must be proportional to the relaxation length and hence to the momentum thickness $\theta$, so $A$ must scale like $U/\theta$; the diffusivity must similarly (cf. the usual scale for the eddy viscosity) scale with $U\theta$ or $w_0\delta$. We therefore put

$$A = aU/\theta, \quad \nu_\tau = w_0 \delta k(\eta), \tag{3.2}$$

where the non-dimensional quantities $a$ and $k$ would, in the simplest version of the model, be taken as universal constants. The number $a$ is simply the ratio of a typical flow time to the characteristic relaxation time of the turbulence.†

It might appear that, in fact, (3.1) and (3.2) virtually decouple the stress equation from the velocity field. However this is not true for (as we shall see in §3.2) it is possible to choose the stress diffusivity so that, under certain conditions, the stress can be obtained through an eddy viscosity – surely a desirable property of the model, as a weakly sheared quasi-homogeneous flow ought to be describable in terms of an eddy viscosity on general statistical-mechanical considerations (see e.g. Kubo 1966).

### 3.2. *Equilibrium solutions of the model equation*

It is obviously important to examine these solutions before a consistent definition of the local equilibrium stress $\bar{\tau}$ is achieved. For a shallow equilibrium wake, the momentum equation is, from (2.4) in I,

$$U\frac{\partial w}{\partial x} - U'y\frac{\partial w}{\partial y} + U'w = -\frac{\partial \bar{\tau}}{\partial y}, \tag{3.3}$$

where the stress $\bar{\tau}$ in equilibrium is governed by the appropriately linearized version of (3.1):

$$\frac{d\bar{\tau}}{dt} \simeq U\frac{\partial \bar{\tau}}{\partial x} - U'y\frac{\partial \bar{\tau}}{\partial y} = \frac{\partial}{\partial y}\left(\nu_\tau \frac{\partial \bar{\tau}}{\partial y}\right). \tag{3.4}$$

By comparing with (3.3), it is easily shown that the stress given by (3.4) is equivalent to that given by an eddy viscosity $\nu_T = \nu_\tau$ if (i) each can be considered a constant, (ii) the pressure gradient is vanishingly small ($\lambda \to 0$) and (iii) the inertia terms in the momentum equation can be linearized.

The equilibrium solutions can now be obtained by the same self-preservation type of analysis as in I, so details (available in Narasimha & Prabhu 1971) will be omitted. The equation governing the stress function $g(\eta) = \tau/w_0^2$ is

$$(kg')' + K_1\eta g - 2K_3 g = 0, \tag{3.5}$$

where

$$K_1 = \frac{1}{w_0}\frac{d}{dx}(U\delta), \quad K_3 = \frac{U\delta}{w_0^2}\frac{dw_0}{dx} = \frac{M}{Uw_0^3}\frac{dw_0}{dx} \tag{3.6}$$

† It is possible to consider $A$ and $\nu_\tau$ as being related to each other, but experiments (§5) indicate a possible departure of $a$ from its standard constant value when the local pressure gradient is very large.

must be constant. The additional condition imposed by the present stress model through $K_3$ implies that equilibrium cannot in general be expected for all $U(x)$. If we take $k(\eta)$ to be a constant, $k_0$ say, (3.5) reduces to an equation encountered earlier by Mellor (1962) and Vasantha & Prabhu (1968). It can be shown that antisymmetric exponentially decaying solutions of this equation exist only when $n = (K_3 + k_0)/k_0$ is an odd integer; the wake development is then given by

$$(U\delta)^2 = M^2(Uw_0)^{-2} = \frac{2(n+1)\,k_0 M}{U^2}\int U\,dx + \text{constant}. \tag{3.7}$$

This must, however, be consistent with the solution of the momentum equation (see equation (2.11) of I)

$$(U\delta)^2 = M^2(Uw_0)^{-2} = 2k_0 M \int \frac{dx}{U(x)} + \text{constant}; \tag{3.8}$$

if $U \sim x^m$ this implies that $m = (n-1)/(n+3)$, i.e. $m = 0, \frac{1}{3}, \frac{1}{2}$, etc.; $0 \leqslant m < 1$. It is easily verified that with the scaling of $A$ given by (3.2) the relaxation term in (3.1) always remains small, so that the solutions do not violate the assumption of equilibrium made in writing (3.3).

### 3.3. *Proposal for equilibrium stress*

The significance of equilibrium solutions obtained only for the isolated values of $m$ derived above must be seriously doubted, especially in view of the assumption that $k(\eta)$ must be a constant. Keeping in mind the experimental evidence discussed in I, we must conclude that the only possible equilibrium flow for a plane turbulent wake is the one that is known to exist, by experiment, at constant pressure (or more precisely for $\lambda \to 0$). The logical choice for $\tau$ is therefore

$$\bar{\tau} = w_0^2\,\bar{g}(\eta), \tag{3.9}$$

where $\bar{g}$ is the equilibrium stress distribution in a constant-pressure wake, for this has the automatic effect of restricting the equilibrium solutions (3.7) of the model to the case $m = 0$.

One can in fact use values of $\bar{g}$ measured experimentally; this is possible because the function $k(\eta)$ of (3.2) can be chosen to yield the measured stress distribution $\bar{g}$ by integrating (3.5):

$$k(\eta) = -\frac{2k_0 \ln 2}{\bar{g}'(\eta)}\left[\eta\bar{g}(\eta) - \int_\eta^\infty \bar{g}(\eta)\,d\eta\right], \tag{3.10}$$

where $k_0$ is a constant determined from experiment. (To find $k$ in terms of the equilibrium velocity distribution $\bar{f}$, one has only to replace $\bar{g}$ by $\eta\bar{f}$ in (3.10).) Values of this function, and also of a standard $\bar{f}(\eta)$ inferred from measurements, are given by Narasimha & Prabhu (1971).

If, therefore, $\bar{\tau}$ and $k(\eta)$ in the model (3.1) are assigned values given by (3.9) and (3.10), we shall have a consistent stress equation which restricts the equilibrium solution to the wake at zero (or small) pressure gradient.

Equation (3.9) defines what may be called the local equilibrium stress, in terms of the true (and *a priori* unknown) defect velocity $w_0$. An alternative definition for $\bar{\tau}$, which may be called the stress with strict equilibrium, would be obtained by putting it equal to $\bar{w}_0^2\bar{g}$, where $\bar{w}_0$ is the self-preserving solution (3.8) for $w_0$. This was considered but abandoned as not being very satisfactory logically, because $\bar{w}_0$ introduces an explicit dependence on $x$ (from the constant-pressure solution) whose significance is doubtful.

We make a final remark here about the stringency of the conditions for the existence of equilibrium. Equilibrium is possible only if the relaxation time $A^{-1}$ is sufficiently small compared with the relevant flow time scales. If there is a pressure gradient, we require $A \gg U'$. The experiments discussed in I suggest that $A = O(10^{-3} \times U/\theta)$; therefore we must have

$$\lambda \ll 10^{-3} \times U\delta/w_0\theta \sim 10^{-3} \times (U/w_0)^2.$$

For $(U/w_0)^2 \sim 10^3$ this requires $\lambda \ll 1$ for equilibrium, as experiments suggest.

We may conclude, therefore, that the model (3.1) is generally consistent with the known qualitative features of both relaxing and equilibrium wakes. It remains to consider how satisfactory it is for quantitative predictions of wake development.

## 4. Solution of the equations

The basic equations to be solved in the present scheme are the momentum equation (3.4) and the stress equation (3.3). In comparing the predictions with the experimental data we need, however, to take account of the observed convergence in the flow, so the equations actually solved incorporate the required modifications described in the appendix.

### 4.1. *The momentum equation*

As noted in I, the defect velocity profiles and the stress distributions exhibit an internal similarity even in non-equilibrium flow; furthermore, although the velocity and stress scales are in general not identical, the length scales for both distributions appear to be practically the same. These facts enable us to obtain a simple and accurate solution of the momentum equation in terms of the (as yet undetermined) stress scale $\tau_0$; the solution, allowing for flow convergence (see appendix), is

$$Uw_0 = \frac{M}{U\delta} = \text{constant} \times \exp\left[-K_1 \int \frac{U\tau_0}{M} dx\right], \tag{4.1}$$

where the constant can be determined from initial conditions. As $\tau_0$ (to be found using the stress equation) involves $w_0$ and $\delta$, an iteration procedure is necessary for completing the solution (4.1). The stress equation may also be solved satisfactorily using an integral approach (Prabhu 1971), but as the equation in question is essentially new it was thought desirable to obtain accurate solutions numerically. Before describing the computational procedure adopted it is convenient to specify the stress equation more closely.

### 4.2. *Parameters in the stress equation*

In the solutions to be presented below we have taken both $a$ and $k(\eta)$ in (3.2) to be constant, chiefly so as to work with the simplest possible model. This implies, in particular, that we are willing to tolerate the observed differences between the measured velocity distribution and the Gaussian. It is not difficult to correct this, using either the function $k(\eta)$ suggested in § 3.3, or a factor taking account of the intermittency of the wake near its edge, as Townsend (1956, p. 161) has done. However, such refinement is unnecessary if we are mainly interested only in predictions of mean flow parameters like $w_0$ and $\delta$.

As a consequence, the stress $\bar{\tau}$ has been taken as

$$\bar{\tau} = w_0^2 \bar{g}(\eta) = (2 \ln 2)\, k_0 w_0^2 \eta \exp(-\eta^2 \ln 2), \tag{4.2}$$

corresponding to the Gaussian velocity distribution. Except in a few calculations made specifically to assess the differences, we have taken $\bar{\tau}$ to be given by the local equilibrium value (4.2) rather than by the strict equilibrium value. The constants $a$ and $k_0$ were chosen to agree with the measurements, as listed in the appendix to I, again with the exception of a few calculations made to test the sensitivity of the results to the choice of parameters.

### 4.3. *The computational scheme*

After incorporating the convergence terms as described in the appendix, the stress equation (3.3) can be written as the parabolic equation

$$\frac{\partial \tau}{\partial x} = a_1 \frac{\partial^2 \tau}{\partial y^2} + a_2 \frac{\partial \tau}{\partial y} + a_3 \tau + a_4, \tag{4.3}$$

where the $a_i$ $(i = 1, 2, 3, 4)$ are given by (see appendix)

$$\left.\begin{aligned} a_1 = \frac{\nu_\tau}{U}, \quad a_2 = \left(\frac{U}{M}\right)' \frac{M}{U} y + \frac{1}{U}\frac{\partial \nu_\tau}{\partial y}, \\ a_3 = A/U, \quad a_4 = -A\bar{\tau}/U, \end{aligned}\right\} \tag{4.4}$$

and in general depend on $w_0$ and $\delta$.

Equation (4.3) has been solved using the Crank–Nicolson finite-difference scheme with suitable difference corrections; the advantages of this procedure are well known (see e.g. *Modern Computing Methods*, National Physical Laboratory, H.M.S.O. 1961).

Figure 3 gives a flow chart for the computational scheme employed. At the beginning of the calculation the stress profile was assumed known at some initial station $x_1$; because of the observed internal similarity it was usually taken as

$$\left.\begin{aligned} \tau(x_1, y) = \tau_0(x_1)\, \bar{g}(y/\delta_1), \\ \tau_0(x_1) = (1+q)\,[w_0(x_1)]^2, \quad \delta_1 = \delta(x_1), \end{aligned}\right\} \tag{4.5}$$

where $\tau_0$ is the stress scale mentioned earlier and $q$ is a number which allows for the possibility of non-equilibrium flow, being zero if the flow was known to be in equilibrium at $x$ . As the finite-difference scheme also requires a knowledge of the

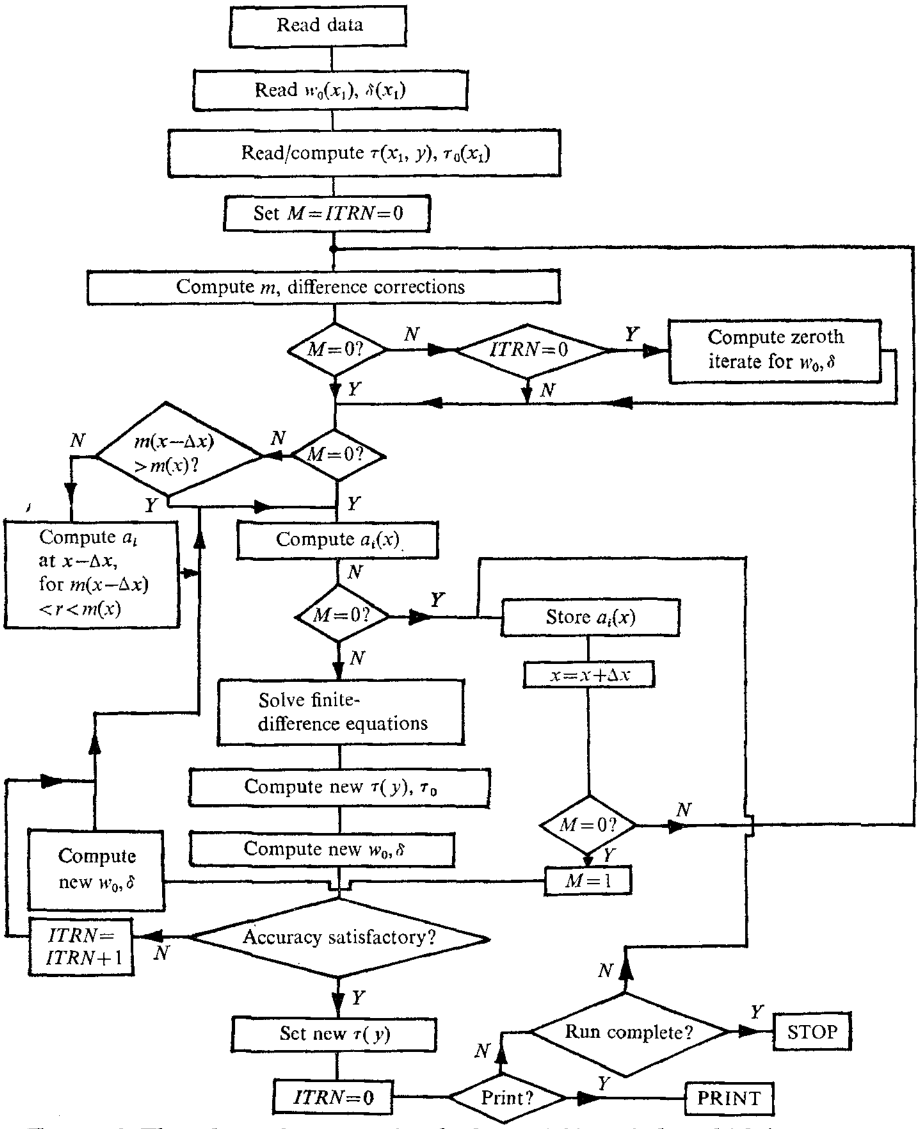


FIGURE 3. Flow chart of computational scheme. $M$ is an index which is zero at the initial station $x_1$ and is unity at all stations downstream. $Y$ = yes, $N$ = no.

$a_i$ at the next step $x+\Delta x$, it is necessary to start with a zeroth iterate for $w_0$ and $\delta$ at $x+\Delta x$. For the first three steps from $x_1$, this was obtained from the strict equilibrium solution (3.8) for $\overline{w}_0$ and $\overline{\delta}$. For $x > x_1 + 3\Delta x$ an extrapolation was made using a four-point Lagrangian formula fitting the calculated solution at the last four points. By using these values to provide a first guess, $\tau$ was calculated at the next step from the Crank–Nicolson scheme. This gave

$$\tau_0(x) = \tau_0(x_1)\,\tau_{\max}(x)/\tau_{\max}(x_1),$$

and hence, from (4.1), new estimates for $w_0$, $\delta$ and $a_i$. These were used for the next iterate and the procedure was repeated until the results from successive iterations agreed sufficiently closely.

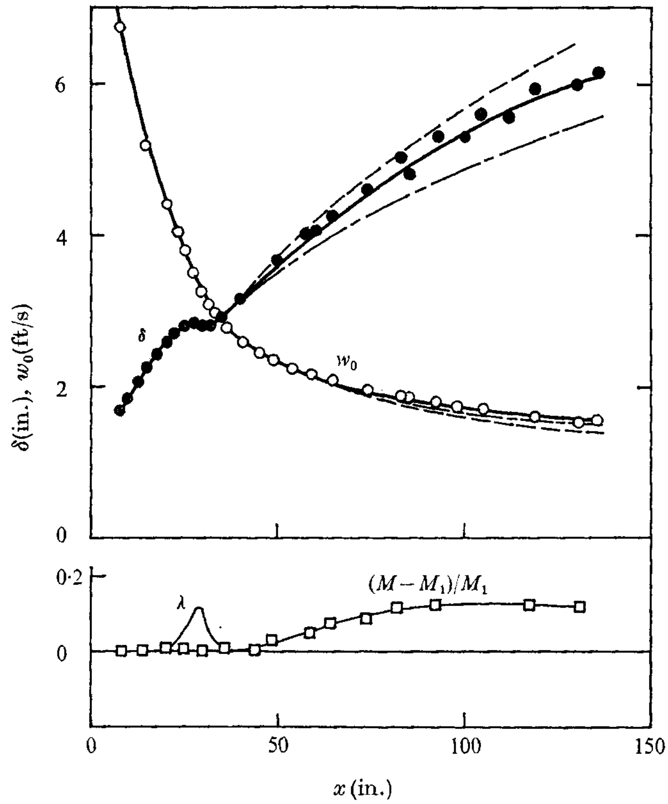


FIGURE 4. Wake development in flow F 2(*b*). Points are experimental measurements; curves in the upper part of the digram show the results of calculations. ———, calculation using local equilibrium values for $\bar{\tau}$ with convergence correction; — — —, calculation using local equilibrium values for $\bar{\tau}$ without convergence correction; – – – –, calculation using strict equilibrium values for $\bar{\tau}$ with convergence correction.

After a few trials, it was found that step sizes of $0{\cdot}1\delta_1$ in $y$ and $2\delta_1$ in $x$ were entirely adequate: for the equilibrium wake this predicted shear stress profiles with an error of less than one in $10^6$. With these step sizes, one iteration was usually enough to provide $w_0$ and $\delta$ to within one in $10^4$. The complete calculation of a flow like any of those listed in table 1, involving say about 50 $y$ steps and 250 $x$ steps, was found to take about $1\frac{1}{2}$ min on a CDC-3600 computer.

More details about the numerical scheme, and a program listing, are available in Prabhu (1971).

## 5. Results

All the flows listed in table 1 have been calculated using the method described above. The two empirical constants needed in these calculations, namely $k_0$ and $a$, have both been determined essentially from the single experiment F 2; $k_0$ from data on wake growth in the equilibrium flow upstream of the (impulsive) pressure gradient and $a$ from the relaxing flow far downstream. The results of the

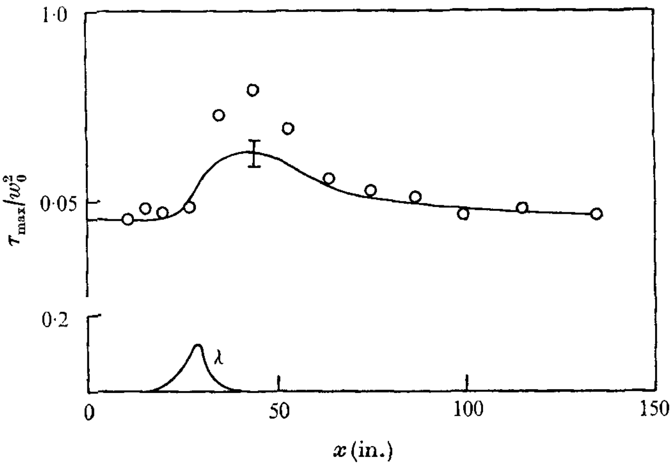


FIGURE 5. Measurements (points) of maximum stress in flow F 2(b) compared with the calculations (solid line) based on the stress equation (3.1). The bar shows the change in prediction if $a$ is changed from $6 \times 10^{-4}$ to $10 \times 10^{-4}$ (lower $a$ gives higher stress) around the standard value we have adopted: $a = 8{\cdot}2 \times 10^{-4}$.

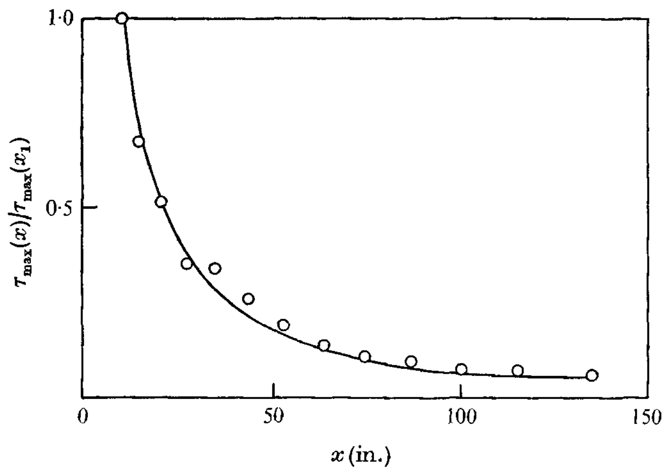


FIGURE 6. Comparison of measured and computed values of $\tau_{max}$ for flow F 2 (b). ———, model solution, $a = 8{\cdot}2 \times 10^{-4}$.

calculation are compared with measurements in a series of diagrams which also show the variations of $\lambda$ and $M$ in each flow.

No results are shown for the flow F 1 because it hardly departs from equilibrium. Figure 4 shows the predictions from the model with the measurements in the flow F 2 (b). Also shown are the results of calculations made both without convergence corrections, using the local equilibrium stress, and with convergence corrections, using either the local or strict equilibrium values for $\bar{\tau}$. It is seen that these different choices hardly affect $w_0$ but $\delta$ is more sensitive; the local equilibrium stress with corrections for convergence shows excellent agreement with experiment.

Figures 5 and 6 show a comparison of the measured maximum stress in the same flow with calculated values. The agreement here is not as good as that for

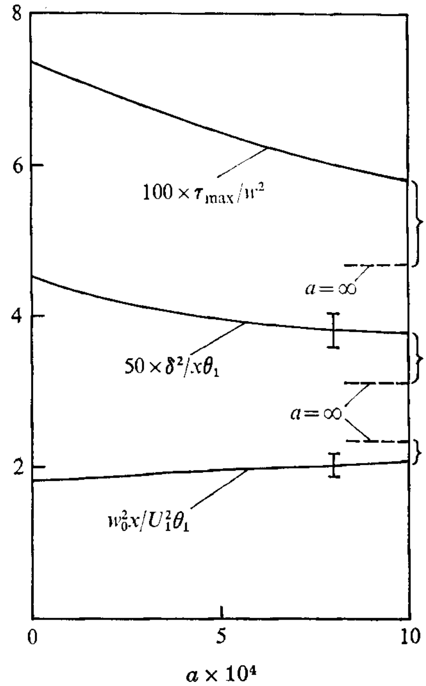


FIGURE 7. Sensitivity of predicted stress, wake defect and thickness to values of the two parameters in the model stress equation. Stress values evaluated at $x = 44$ in., $w_0$ and $\delta$ at $x = 132$ in. On the curves $k_0 = 0{\cdot}065$. Bars show changes in prediction for change in $k_0$ from 0·06 to 0·07 ($\delta$ increases and $w_0$ decreases as $k_0$ increases).

mean flow parameters. There are, however, several plausible reasons for this. The calculations have been based on the assumption (4.2), which cannot be strictly true and is likely to affect the stress distribution near and beyond $\eta \gtrsim 1{\cdot}0$, and in particular the value of $\tau_{max}$. In this region, however, the stress gradient $\partial\tau/\partial y$ is small; as it is only the gradient which appears in the momentum equation, mean flow parameters like $w_0$ and $\delta$ can still be predicted satisfactorily. It is also possible that some of the discrepancy may be due to the neglected normal stress terms in the momentum equation. Nevertheless, the 'freezing' of the stress while the wake is being subjected to pressure gradient, pointed out in I, suggests that $a$ might depend on the strain ratio, decreasing rapidly to zero as (say) $\lambda$ increases. Note that the ordinate variable in figure 5 is proportional to $\nu_T/w_0\delta$, and shows stronger variations than the stress itself; the eddy viscosity is therefore harder to model faithfully.

Figure 7 shows that the results of the calculations are not very sensitive to slight changes in $a$ or $k_0$. Figure 8 shows results for the flow F 3. Also shown here, for comparison, are the predictions of classical self-preserving theory, with and without convergence corrections. Figure 9 shows results of an early experiment on the wake behind a circular cylinder. In this case, the wake was almost certainly not in equilibrium at the initial station (50 diameters downstream of cylinder) and so calculations were made for several different values of $q$. It is seen that with

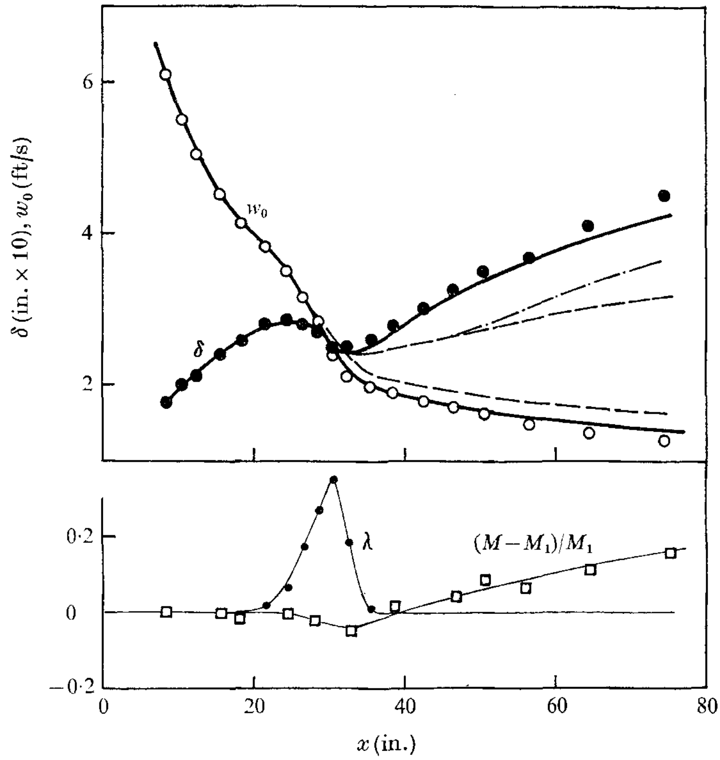


FIGURE 8. Comparison between measured and calculated wake development in flow F3. – – – –, equilibrium solution; — · —, equilibrium solution for $\delta$ corrected for convergence from (A 3); ———, calculation using local equilibrium stress with convergence correction.

$q = 0{\cdot}2$ agreement between theory and experiment is very good; changes in $q$ again affect $\delta$ more than $w_0$.

Figures 10($a$) and ($b$) show the results for flows with adverse and mixed pressure gradients. Unfortunately it was found to be difficult to reduce the momentum imbalance much below 30% at the last station in the adverse pressure gradient experiment A 1; it may be recalled that this experiment was conducted in a small tunnel. The flow M 1, in which a sharp fall in pressure is followed by a slightly more gradual rise, is perhaps the most severe test of the model; it is seen that the predictions from the model faithfully reproduce the measured kinky distributions† of $w_0$ and $\delta$.

Finally we present an analysis of flows studied by Keffer (1965, 1967). Here the wake behind a circular cylinder was subjected to disortion in a duct of constant cross-sectional area (so that there was no pressure gradient). Keffer was seeking possible equilibrium flows; but, by using Keffer's data to find $M = M(x)$ and

† If $\lambda w_0^2/\tau_0$ is large (this needs only moderate $\lambda$ as $w_0^2/\tau_0$ is of order 10) the stress term in (3.3) can be ignored, and both $U\delta$ and $Uw_0$ are then constant, by (4.1). Although this 'ideal-fluid' approximation is not quantitatively satisfactory in the present experiments, it indicates the physical mechanism responsible for the observed thinning of the wake during acceleration in the flows F 3 and M 1.

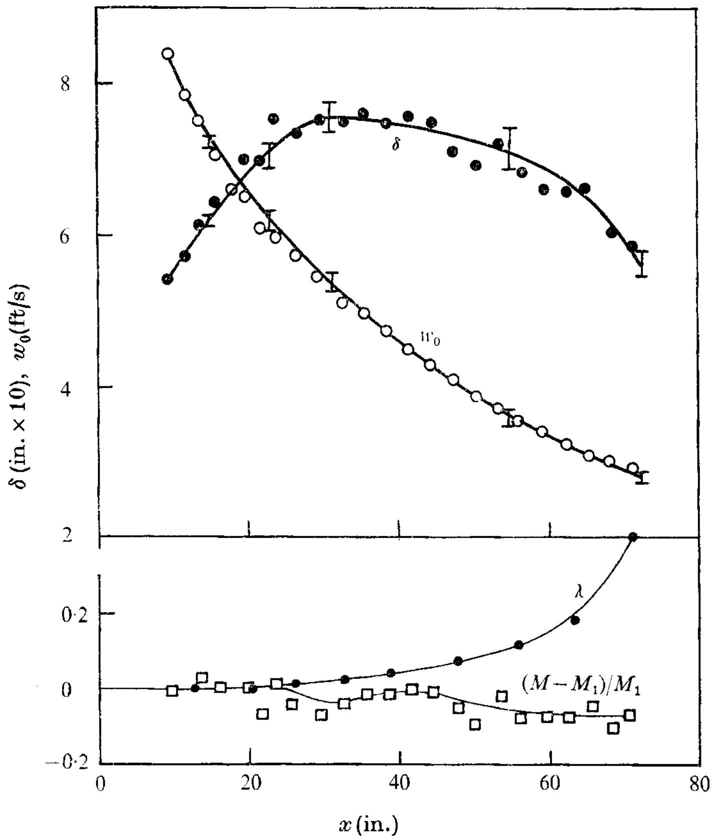


FIGURE 9. Comparison between measured and calculated wake development, flow F 4. On the curves (from the theory) the initial value of $q$ is taken as 0·2. Bars show change in prediction as $q$ increases from 0·1 to 0·3 ($\delta$ increases, $w_0$ decreases).

hence the local convergence, the flow can be analysed along the same lines as the other flows we have been discussing. The results shown in figure 11 correspond to the case (Keffer 1965) when the distortion compresses the wake in the normal direction. Computations were made using the methods indicated in §4.3. They agree quite well with the measurements except over the last 10 in. or so; the disagreement here could well be due to the existence of a pressure gradient, noted by Keffer, in the neighbourhood of the transition from the distorting duct to a uniform channel in his experimental set-up.

Figure 12 compares the results of similar calculations with the later experiments of Keffer (1967) where the distortion stretches the wake in the normal direction. The agreement with the experiments is again quite good. It would appear, therefore, that the effect of distortion on the turbulent wake in these experiments might merely be to produce departures from plane flow; it is not necessary to postulate changes in the turbulent structure (cf. Bradshaw 1971) with either kind of distortion to explain the observed flow development.

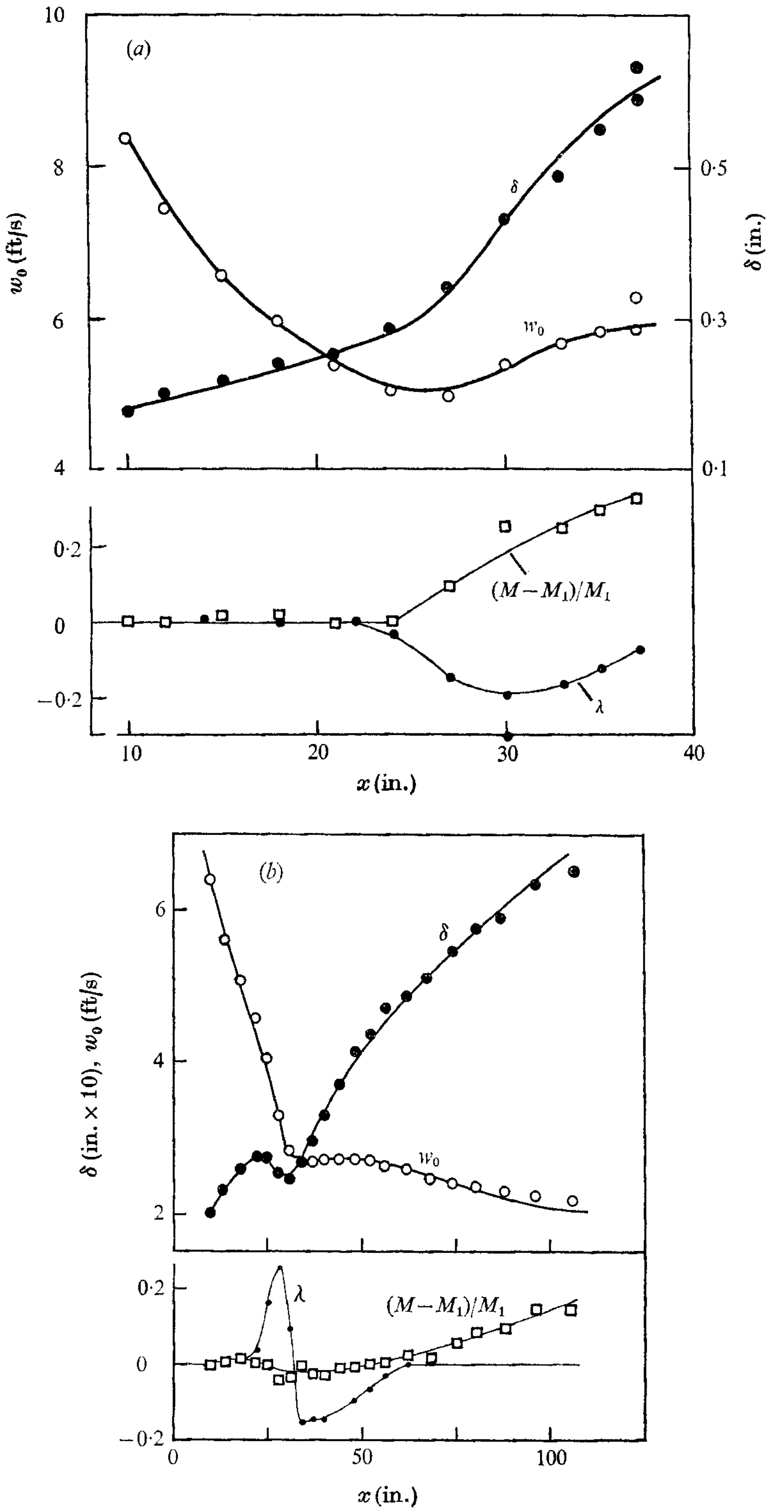


FIGURE 10. Comparisons between measured and calculated wake development. Points represent measurements; solid lines in the upper parts of the diagrams are from calculation. (a) Flow A 1. (b) Flow M 1.

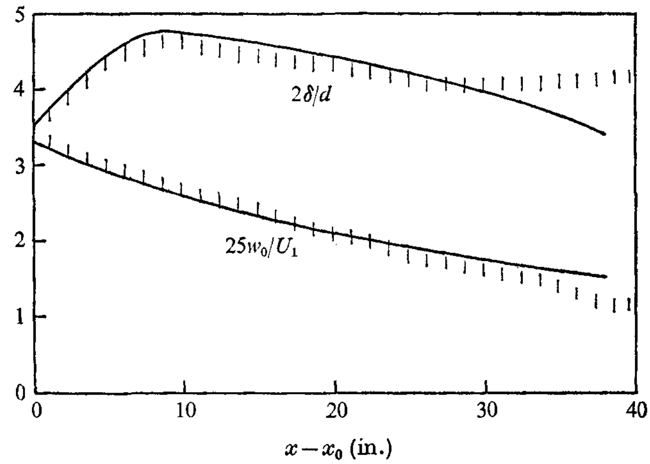


FIGURE 11. Comparison between measured and calculated wake development in the distorted wake studied by Keffer (1965). Diameter of the cylinder $d = \frac{3}{16}$ in.; distance of the beginning of distortion from the cylinder = 10 in. ———, calculations using $k_0 = 0{\cdot}065$, $q = 0$.

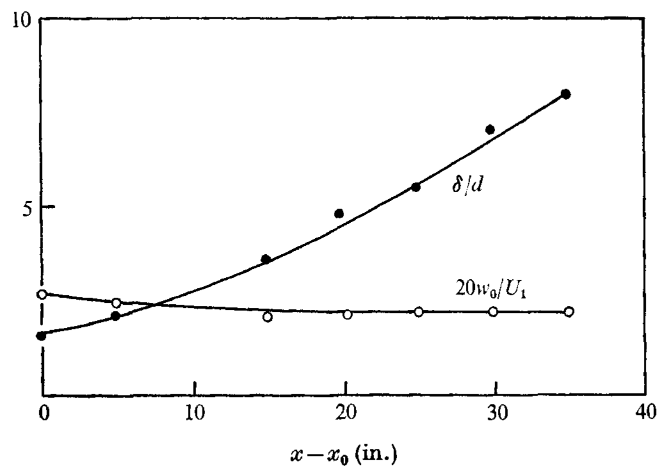


FIGURE 12. Comparison between measured and calculated flow development in the distorted wake studied by Keffer (1967). Diameter of the cylinder $d = \frac{1}{8}$ in.; distance of the beginning of distortion from the cylinder = 20 in. ———, calculations using $k_0 = 0{\cdot}065$, $q = 0$.

## 6. Conclusions

It has been shown that the development of wakes subjected to arbitrary pressure gradients, and even to (relatively mild) distortion, can be described in terms of the concepts of equilibrium and relaxation, both being capable of quite precise definition. There is some evidence that when pressure gradients are extremely large the stress 'freezes', but this phenomenon, presumably characterizing 'rapid distortion', needs further investigation. A more fundamental understanding of all these processes can only be provided by detailed studies of energy and stress balance, but it is useful to be able to classify flow behaviour into a few recognizable (even if gross) phenomena.

The wake, which is the only flow studied here, has a turbulent energy balance dominated by advection and so may be expected to have a longer memory than a production-dominated flow. However there is a well-known resemblance between the outer part of a turbulent boundary layer and a wake (Townsend 1956; Coles 1956), and some of our general conclusions ought to be valid for a wider class of flows, with suitable modifications to allow for the coupling that is known to exist between the inner and outer flows in the boundary layer. Thus, it may be expected that self-preserving solutions of the mass and momentum equations can in general be observed only if the relaxation time for the turbulent flow is small compared with an appropriate flow time, or if the pressure gradient is sufficiently small.

We finally note that the numerical approach adopted in the present work to solve the equations should not always be necessary; work now in progress has shown that approximate solutions can be obtained by simpler methods. Indeed one of the advantages of the model used here is that it is simple enough to be tractable, at least in some special cases, without resort to heavy computation.

## Appendix. Convergence corrections

When measurements in any of the experiments reported here showed that the two-dimensional momentum integral equation was not strictly obeyed we applied 'convergence corrections' (to either measured or calculated values) along the lines proposed by Bradshaw & Ferriss (1965) for turbulent boundary-layer flows. The correction attributes the apparent momentum imbalance to a slow convergence of streamlines in the transverse (i.e. $x, z$) plane towards the axis of the flow. To a first approximation such convergence may be considered to have a centre at some (large) distance $x_c$ downstream. The resulting influx of fluid into the plane of symmetry $(x, y)$, of amount $u/(x_c - x)$ per unit volume, alters the momentum equation (3.4) to

$$U\frac{\partial w}{\partial x} - \left(U' - \frac{U}{x_c - x}\right) y \frac{\partial w}{\partial y} + U' w = -\frac{\partial \tau}{\partial y} \qquad \text{(A 1)}$$

for a small defect wake. The corresponding momentum integral equation is now

$$\frac{d\theta}{dx} + \frac{U'}{U}(H+2)\,\theta = \frac{\theta}{x_c - x}.$$

Integrating for a small defect wake (with $H \simeq 1$ and $\theta$ proportional to $w_0\delta/U$ for similar defect velocity distributions) finally gives

$$M = U^2 w_0 \delta = \text{constant}/(x_c - x), \quad \text{or} \quad x_c - x = M/M',$$

where $M' = dM/dx$. Putting this in (A 1) yields the corrected momentum equation

$$U\frac{\partial w}{\partial x} - (U/M)'\, My \frac{\partial w}{\partial y} + U'w = -\frac{\partial \tau}{\partial y}. \qquad \text{(A 2)}$$

We may now find the self-preserving solutions of (A 2), using the same method of analysis as in I. Again it is easily shown that such solutions exist for arbitrary $U(x)$, but the wake development is now given by a slightly modified version of (3.8):

$$\frac{(U\delta)^2}{M^2} = \frac{1}{(Uw_0)^2} = 2K_1 \int \frac{dx}{U(x)\,M(x)} + \text{constant}. \tag{A 3}$$

The corrected equilibrium solution shown in figure 7 was obtained from (A 3).

If we follow the same procedure as for the momentum equation, replacement of $yU'$ by $yM(U/M)'$ gives the corrected stress equation as

$$U\frac{\partial \tau}{\partial x} - (U/M)'\,yM\frac{\partial \tau}{\partial y} = A(\bar{\tau}-\tau) + \frac{\partial}{\partial y}\left(\nu_\tau \frac{\partial \tau}{\partial y}\right). \tag{A 4}$$

For given $M(x)$, (A 2) and (A 4) govern the wake development.

A fairly simple correction, and incidentally a useful integration of the momentum equation, can be obtained if we are willing to assume that the flow, even when not in equilibrium, possesses the internal similarity mentioned in I. Thus, if we put

$$w/w_0 = f(\eta), \quad \tau/\tau_0 = g(\eta), \tag{A 5}$$

where $\tau_0$ is a stress scale, it can be shown, using the same kind of analysis as in I, that the solution of (A 2) can be reduced to a quadrature in terms of $\tau_0$:

$$Uw_0 = \frac{M}{U\delta} = \text{constant} \times \exp\left[-K_1 \int \frac{U\tau_0}{M}\,dx\right]. \tag{A 6}$$

This 'solution' is in fact found to be quite accurate, which is not surprising as experiment shows that the assumptions (A 5) are very good. Of course $\tau_0$ itself depends on $w_0$ and $\delta$, through the stress model, so that (A 6) is still an integral equation rather than a closed solution.

Now in the present experiments, the departure of $M(x)$ from an initial (nearly constant) value $M_1$ is quite small, and furthermore occurs relatively far downstream (see figures 4–10). The change in the value of the integral in (A 6) or (A 3) due to the departure of $M$ from $M_1$ is therefore particularly small, being of the order of only a few per cent even at the last measuring station in the present experiments. We may conclude immediately that the three-dimensionality hardly affects the prediction of $w_0$, and alters the prediction of $\delta$ in proportion to the local value of $M(x)$.

This is a fairly general conclusion, for which the basic reason is that the equation of motion along the axis of the flow, and hence $w_0$, is unaffected by the convergence. As the first equation in (A 3) is always valid because of the universal similarity of wake defect profiles, it follows that in general $\delta$ may be expected to vary directly like $M$. Experimental data on wake development may therefore be corrected for convergence, in a relatively simple way, by merely multiplying the measured $\delta$ by the factor $M_1/M$.

REFERENCES

BRADSHAW, P. 1969 *N.P.L. Aero Rep.* no. 1285.

BRADSHAW, P. 1971 *J. Fluid Mech.* **46**, 417.

BRADSHAW, P. & FERRISS, D. H. 1965 *N.P.L. Aero Rep.* no. 1145.

BRADSHAW, P., FERRISS, D. H. & ATWELL, N. P. 1967 *J. Fluid Mech.* **28**, 593.

COLES, D. 1956 *J. Fluid Mech.* **1**, 191.

KEFFER, J. F. 1965 *J. Fluid Mech.* **22**, 135.

KEFFER, J. F. 1967 *J. Fluid Mech.* **28**, 183.

KUBO, R. 1966 *Rep. Prog. Phys.* **29**, 255.

MELLOR, G. 1962 *J. Appl. Mech.* **29**, 589.

NARASIMHA, R. 1969 *Curr. Sci.* **38**, 47.

NARASIMHA, R. & PRABHU, A. 1971 *I.I. Sc. Aero. Rep.* 71FM 3.

NARASIMHA, R. & PRABHU, A. 1972 *J. Fluid Mech.* **54**, 1.

NASH, J. F. & HICKS, J. G. 1969 In *Computation of Turbulent Boundary Layers. Proc. AFORS-IFP-Stanford Conference.* Thermosciences Division, Department of Mechanical Engineering, Stanford.

NEE, V. W. & KOVASZNAY, L. S. G. 1969 *Phys. Fluids*, **12**, 473.

PRABHU, A. 1971 Ph.D. thesis, I.I. Sc., Bangalore.

REYNOLDS, A. J. 1962 *J. Fluid Mech.* **13**, 333.

TOWNSEND, A. A. 1956 *The Structure of Turbulent Shear Flow.* Cambridge University Press.

VASANTHA, S. & PRABHU, A. 1968 *A.I.A.A. J.* **6**, 2224.